TITLE: NAMPT activity plays a key role in driving autoimmune processes that characterise type 1 diabetes development in mice

AUTHORS: Daniel Egbase[1], Sophie R. Sayers[1], Naila Haq[1], Jithu Varghese [1], Sreya Bhattacharya[1,2], Jay Kynaston[1], Ella L. Hubber[1], Lorna Smith[1], Timothy J. Pullen[1], Henry Gerdes[3], Vivian K. Lee[1], David Hopkins[1], Minh Zhao[1], Yee Cheah[1], Joshua Greally[4], Sam Butterworth[4], James A Pearson[5], Gavin Bewick[1], Shanta Persaud[1] and Paul W. Caton[1].

[1] Department of Diabetes, School of Cardiovascular and Metabolic Medicine & Sciences Faculty of Life Sciences and Medicine, King's College London, UK

[2] Institute of Diabetes and Regeneration Research, Helmholtz, Munich, Germany

[3]Cell Signalling and Proteomics Group, Centre for Genomics & Computational Biology, Barts Cancer Institute, Queen Mary University of London, Charterhouse Square, London, UK

[4] Division of Pharmacy and Optometry, Faculty of Biology, Medicine and Health, University of Manchester, UK

[5] Division of Infection and Immunity, Cardiff School of Medicine, Cardiff University, Cardiff

Corresponding Author: Paul W. Caton, Department of Diabetes, School of Cardiovascular and Metabolic Medicine & Sciences, King's College London, Hodgkin Building, Guy's Campus, London, SE1 1UL; Email, paul.w.caton@kcl.ac.uk. ORCID ID: 0000-0003-0902-0676

Word Count: 5823

Abstract

Objective: Type 1 diabetes (T1D) is characterised by destruction of pancreatic beta cells by islet-infiltrating cytotoxic lymphocytes, and elevated intra-islet secretion of pro-inflammatory cytokines. However, the underlying pathophysiological mechanisms remain incompletely understood. We hypothesise that abnormal elevation of islet NAD, via activation of NAMPT, plays a key role in driving islet autoimmune processes in T1D, and that conversely, NAMPT inhibition may be an attractive therapeutic approach for T1D.

Methods: Islets were isolated from non-diabetic CD1 mice or obtained from human islet donors and exposed to pro-inflammatory cytokine cocktail (IL-1β, TNFα and IFNγ) +/- NAMPT inhibitor. Beta-cell function was determined by static glucose-stimulated insulin secretion. Islet apoptosis was determined by caspase 3/7 activity. Islet cell differential gene expression was assessed via bulk-RNA sequencing. Diabetes was induced in CD1 mice via multiple low dose streptozotocin (MLDS) injection. MLDS mice were then administered FK866 (10 mg/kg; IP) or saline equivalent for 16 days. Ambient blood glucose was measured every 2-3 days. Beta-cell function was assessed by measurement of serum insulin and c-peptide levels. Insulin content was assessed by flow cytometry. Intra-islet immune cell infiltration, as well as immune cell proliferation and cytokine production were assessed via flow cytometry. For migration assays, islets were isolated from BALB/c mice dispersed and reaggregated into reformed islets. $CD8^+$ cells were isolated from splenocytes derived from NY8.3 NOD mice migration of immune cells was assessed using a transwell culture protocol.

Results: NAMPT inhibition with FK866 or compound 17 protected mouse and human islets against cytokine-mediated beta cell dysfunction and death. RNAseq revealed that inhibiting NAMPT blocked pro-inflammatory cytokine-mediated gene expression linked to pro-inflammatory responses and leukocyte migration. FK866 improved glycaemic control and beta-cell function in MLDS mice. FK866 also reduced proportions of islet-residing TNFα producing $CD4^+$T-cells and $F4/80^+$macrophages, proliferation of spleen-derived $CD4^+$ and $CD8^+$T-cells, and proliferation of islet-derived $CD4^+$T-cells and $F4/80^+$macrophages. Finally, FK866 was able to block pro-inflammatory cytokine-mediated migration of cytotoxic $CD8^+$T-cells into reformed islets.

Conclusions: This data supports a key immunomodulatory role for NAMPT in islet autoimmunity. NAMPT inhibition may represent a novel therapeutic approach for T1D.

Keywords

Beta cell, NAMPT, nicotinamide phosphoribosyltransferase, NAD, inflammation, insulitis, T-cell, macrophage, type 1 diabetes

Introduction

Type 1 diabetes (T1D) is an autoimmune disorder characterised by auto-reactive immune cell-mediated destruction of insulin-producing pancreatic beta cells. The precise triggers that initiate pathogenesis of T1D remain unclear, with both genetic susceptibility and/or environmental triggers reported to prime autoimmune events in affected individuals (1-5). Autoimmune events in T1D are characterised by the generation and islet infiltration of islet-reactive $CD4^+$ and $CD8^+$T-cells, in a process known as insulitis (6). Furthermore, increased islet antigen presentation towards islet-infiltrating T-cells leads to elevated numbers of activated lymphocytes. In their activated state, cytotoxic $CD4^+$ and $CD8^+$T-cells secrete pro-inflammatory cytokines (such as IL-1β, TNFα and IFNγ) within the intra-islet environment (7-9). This ultimately results in autoimmune destruction of the beta-cell, consequent lack of insulin secretion and onset of the hyperglycaemia.

There are a several of issues surrounding the current standard-of-care for T1D, including hypoglycaemia associated with exogenous insulin therapy and poor graft survival following islet transplantation (10-13). Recently, a focus has been placed on immunomodulatory interventions designed to reduce islet inflammation, with teplizumab, an anti-CD3 mAb which can delay development of T1D, recently approved. However, additional therapeutic options are required, and the precise pathophysiological mechanisms which drive immunological and inflammatory process within the islet in T1D remain incompletely understood.

One candidate as a regulator of these process is nicotinamide phosphoribosyltransferase (NAMPT). NAMPT is well characterised as the rate-limiting enzyme in the NAD salvage pathway, where it catalyses the conversion of nicotinamide (NAM) to nicotinamide mononucleotide (NMN). NMN is subsequently converted to NAD by NMN adenynyltransferase (NMNAT1 – 3) enzymes (14). NAD+ metabolism facilitates homeostasis of the innate and adaptive immune response (15). However, accumulating evidence indicates that NAMPT activity, potentially via its effects on intracellular NAD+ levels, plays a role in the dysregulation of immunomodulatory processes and onset of inflammation. Crucially, many of these changes are recognised as key pathogenic events that take place during T1D development.

For instance, NAMPT activity reportedly induces TNFα production in mouse and human inflammatory cells (16) and can indirectly lead to T-cell activation and production of IFNγ in mature T-cells (17-19). Furthermore, NAMPT inhibition leads to decreased proliferation, reduced IFNγ and TNFα production, and autophagy-mediated T-cell death. Interestingly, inactive T lymphocytes are spared from this effect (20). NAMPT activity is also reportedly required for activation of pro-inflammatory M1 macrophages, and NAMPT inhibition downregulates TNFα expression in M1 macrophages and skews macrophages towards an anti-inflammatory M2 phenotype (21 – 24). Consistent with these findings, a key role for NAMPT activity in pathogenesis of auto-immune conditions such as Inflammatory Bowel Disease, arthritis and autoimmune encephalomyelitis has been reported (20, 24).

Together, the evidence outlined above strongly suggests a potential role for NAMPT activity in the pathophysiology of islet autoimmunity and beta-cell destruction and supports detailed investigation of NAMPT inhibition as a target for T1D treatment.

Specifically, we hypothesised that NAMPT inhibition may reduce insulitis, intra-islet cytokine production and immune cell activation in T1D. To investigate this, we examined the anti-diabetic effects of two separate potent NAMPT inhibitors, FK866 (25,26) and compound 17 (27), in the multiple-low dose streptozotocin (MLDS) type 1 diabetes mouse model (28) and in isolated mouse and human islets treated with pro-inflammatory cytokines.

Research Design and Methods

MIN6 cell culture

MIN6 cells were cultured at 37°C in DMEM (25 mmol/l glucose; 2 mmol/l glutamine, 10% FBS (vol./vol.), 100 U/ml penicillin, 100 µg/ml streptomycin) and treated with FK866 or compound 17 (24 h) prior to NAD and NMN measurements.

NMN and NAD+ Measurement

NMN was measured in a cell-free environment or in MIN6 β-cells using a fluorometric assay based on previous described methodology (29,30). For cell-free experiments, reaction mixtures were prepared in triplicate containing the following: 1ml of Reaction Buffer (made up of PRPP (Sigma, UK), 2 mM ATP, 0.02% bovine serum albumin (BSA), 2 mM dithiothreitol (DTT), 12 mM MgCl2, and 50 mM Tris–HCl (pH 7.5)), 2ug/ml recombinant NAMPT and FK866 (5 – 20 nM) or compound 17 (50 – 200 nM). For NMN measurements in cells, MIN6 were maintained in monolayer culture. Then, 20,000 MIN6 β-cells were extracted with 100 µl of 1 mol/L perchloric acid and then neutralized by addition of 330 mL of 3 mol/L K2CO3. This was followed by incubation at 4 °C for 10 min, and centrifugation at 12000 x g for 15 min at 4 °C, with the supernatant retained. 50 ml of samples (reaction mixtures or cellular samples) and of standard solutions of NMN (50 ml; 25 – 200 mmol/l) were subsequently derivatised by addition of 20 ml of 1 mol/L KOH and 20 ml acetophenone (Sigma, Poole, UK) followed by incubation at 4°C for 15 min. 90 ml Formic acid was then added, and the solution incubated for 10 min at 37°C, producing a highly fluorescent compound. 150 ml of samples or standards were then added into a 96-well plate fluorescence was detected on a SpectraMax i3x plate reader with excitation and emission wavelength of 382 and 445 nm, respectively. NAD was measured by specific colorimetric assays, according to manufacturer's instructions (Sigma-Aldrich).

Pancreatic islet isolation

Mouse islets were isolated from 8-week-old non-diabetic CD1 mice between 10:00 and 11:00 hours, as previously described (31). Pancreata were inflated with 1mg/mL collagenase solution (Sigma-Aldrich, Poole, U.K.) followed by density gradient separation (Histopaque-1077; Sigma-Aldrich). Human islets were isolated from heart-beating non-diabetic donors (31) at the King's College Hospital Human Islet Isolation Unit, with the appropriate ethical approval (KCL HI-RTB; 20/SW/0074). Isolated islets were maintained in supplemented RPMI at 37 °C and 5% CO_2 in a humidified atmosphere for up to 24 hours prior to experimental treatment.

Pancreatic islet treatment

For analysis of cytokine-mediated effects, ~60 mouse islets were incubated with a cocktail of pro-inflammatory cytokines (0.05 U/ml Il-1β, 1 U/ml TNFα and IFNγ to create a 1 ng/ml cocktail) with or without either FK866 (10 – 40 nM) or compound 17 (50 – 400 nM). Separately, islets were also treated with FK866 (10 nM) or compound 17 (200nM) alone for 24 h. For proliferation assays,

~100 isolated mouse islets were incubated with 20 μM EdU in RPMI (supplemented with 2% FBS, 2 mM L-glutamine and 100 U/ml penicillin/ 0.1 mg/ml streptomycin) for 72 h.

Static glucose-stimulated insulin secretion

For static insulin secretion, mouse CD1 or human islets were pre-incubated in a physiological salt solution containing 2mM glucose. Groups of 5 size-matched islets were then further incubated at 37°C for 1 h in salt solution and 2 or 20 mmol/l glucose. Secreted insulin was measured using an in-house I125 radioimmunoassay (32).

Islet apoptosis

Human and mouse islet cell apoptosis was determined by the Caspase-Glo 3/7 luminescent assay (Promega, Southampton, UK).

Bulk RNA Sequencing Analysis

Total RNA was extracted from ~150 islets per mouse, according to the manufacturer's instructions (RNeasy Mini Kit, Qiagen, UK). Total RNA concentration and purity from extracted mouse islet RNA was quantified by loading 1 μl samples onto a NanoDrop (ND-1000, Thermo Fisher Scientific, Hemel Hempstead, UK) spectrophotometer. 100ng total RNA from each sample was used as input to generate library for RNAseq. RNAseq libraries were prepared using NEBNext Ultra II Directional RNA Library Prep kit (New England Biolabs, Hertfordshire, UK. Cat.no: E7760) following manufacturer's recommendations. In brief, mRNA was isolated using the Poly-A mRNA magnetic isolation module (E7490) (New England Biolabs, Hertfordshire, UK). Isolated mRNA was enzymatically fragmented prior to cDNA synthesis. Each sample was then tagged with a single index that was unique to the sample. cDNA library was amplified by PCR for 12 cycles. The resulting library was purified using Agencourt AMpure XP beads (Beckman Coulter, Buckinghamshire, UK). Library quality was assessed using a Bioanlyzer 2100 and DNA High Sensitivity kit (Agilent). Library fragment size distribution was determined using Agilent 2100 expert software. Library concentration was determined by qPCR using NEBNext Library Quant Kit for Illumina (New England Biolabs (NEB), Hertfordshire, UK. Cat.no: E7630). Libraries were pooled at equal molar ratio and sequenced using an Illumina NovaSeq 6000 at 150bp paired end with an approximated depth of 25 million reads per sample.

Diabetic mouse models

Diabetes was induced using a well characterised multiple-low dose streptozotocin (MLDS) methodology (33). 4-6 week old CD1 mice (Charles Rivers, UK) were randomly assigned into four groups: non-diabetic control group (citric acid buffer (CAB)^{Saline}), diabetic control group (MLDS^{Saline}), FK866-treated diabetic group (MLDS^{FK866}), and vehicle (5% in DMSO in saline)-treated diabetic group (MLDS^{Vehicle}) For MLDS administration, age and weight (26 – 33g) matched animals were administered 40 mg/kg/body weight STZ (IP; Bio-techne, Bristol, UK; dissolved in CAB, pH 4.5) or CAB equivalent, for 5 consecutive days (days 1 – 5). For FK866 administration, FK866 (10 mg/kg body weight; IP) or DMSO control was administered for 16 days (Days 7-22).

Mice were housed in 12 h light/dark cycle, temperature-controlled conditions with *ad libitum* access to standard mouse chow (Envigo) and water. Procedures were performed in accordance with UK Home Office regulations (Animal Scientific Procedures Act, 1986).

Diabetes evaluation

Diabetes was defined by presence of hyperglycaemia (ambient blood glucose levels > 13.8 mM) over 3 consecutive days in *ad libitum fed* animals (28). Ambient blood glucose levels were measured every 2 – 3 days at 10 am. Blood samples were taken from the tail tip. Capillary blood glucose levels (mM) were determined using an Accucheck glucose meter (Roche Diagnostics, UK).

Serum Insulin and C-peptide

Overnight fasted mice were administered 2 g/kg body weight 30% glucose solution (IP). After 30 min, mice were culled, and blood was collected. Plasma insulin (Mercodia, Sweden) and C-peptide (ALPCO, United States) were measured by specific ELISA.

Histological examination of pancreas

Whole pancreases were excised and fixed in 4% paraformaldehyde for 24 h prior to tissue processing (Leica TP 1020, Leica Biosystems, Germany) and embedding in paraffin wax 5 µm paraffin sections were melted briefly on a hot plate before the slides were dewaxed using xylene and then rehydrated using solutions of decreasing ethanol gradient (100%–70%). The staining procedure was as follows: 5 min immersion in haematoxylin, 5 min in running water, three to five dips in acid alcohol, 2 min in running water, five dips in eosin and then 2 further minutes in

running water. After staining, the sections were dehydrated in an increasing ethanol gradient (70%–100%). Finally, the sections were immersed in xylene for 7 min before being mounted. Slides were imaged with a bright field channel on a microscope (Olympus BX40). A minimum of 60 islets per mouse (three mice per group) were scored for insulitis. Histological analysis of immune cell infiltrates in pancreatic islets was performed in blinded fashion by an independent observer (JK).

Islet dissociation prior to flow cytometric analysis

Islets were isolated from MLDS mice, washed in PBS and dissociated with TrypLE Express (1 ml/100 islets) for 10 min at 37 °C, triturating every 5 min for 10 s. After washing with DMEM (supplemented with 10% FBS), then PBS, samples were transferred to round bottom tubes and kept on ice.

Spleen dissociation and treatment prior to flow cytometric analysis

MLDS mouse splenocytes were isolated as previously described (34). On the day of sacrifice, spleens were removed, placed on ice in Hanks' Balanced Salt Solution and mechanically disrupted using forceps. The cell suspensions were centrifuged at 1500 rpm (4°C) for 5 minutes and erythrocytes were lysed by suspension of the pellets in 5 ml of ACK (Ammonium-Chloride-Potassium) Lysing Buffer (ThermoFisher Scientific, Altrincham, UK). The cell suspensions were then incubated at room temperature for 10 minutes, followed by centrifugation. The supernatants were discarded, and the pellets were washed twice with HBSS and resuspended in supplemented RPMI. An aliquot of cell suspension was mixed with 0.4% trypan blue solution (Sigma-Aldrich). Through the trypan blue exclusion method, and using a haemocytometer chamber the cells were counted. 1 × 106 cells/ml of cells were seeded on P24 round-bottom plates and cultured (37 °C 5% CO_2) in 10 μM EdU for 24 h. To detach from the flask, cells were then incubated in a solution of trypsin/EDTA (0.1%/0.02%) for 2 min in an incubator at 37 °C, prior to addition of DMEM. After centrifugation at 1000 rpm for 2 min, the spleen cell pellet was re-suspended in fresh DMEM and kept on ice for flow cytofluorimetry analysis.

Flow cytometric analysis

To assess viability, single-cell suspensions were stained with LIVE/DEAD™ Fixable Blue Dead Cell Stain (Thermo Fisher Scientific). To assess surface immune cell markers, single-cell suspensions were incubated with anti-mouse CD4, CD8 and F4/80 fluorochrome-conjugated monoclonal

antibodies (all 1:50 dilution), or with isotype-matched controls (Becton Dickinson, Wokingham, UK) for 45 minutes at RT. Following staining, cells were fixed and permeabilized with Intracellular Fixation & Permeabilization Buffer Set (Thermo Fisher Scientific, UK). To assess for proliferative cells, Click-iT EdU Flow Cytometry Cell Proliferation Assay (Thermo Fisher Scientific, Hemel Hempstead, UK) was used according to manufacturer's instructions. Briefly, cells were resuspended in 100 µL of 1X Click-iT® saponin-based permeabilization, then 0.5 mL of Click-iT® reaction cocktail was added to each sample for 30 minutes at room temperature, protected from light. Samples were washed twice with 1 mL of 1X Click-iT® saponin-based permeabilization and wash reagent, followed by resuspension in eBioscience™ Flow Cytometry Staining Buffer (Thermo Fisher Scientific, UK). To assess other intracellular proteins, single-cell suspensions were incubated with anti-mouse insulin (1:100), IFNγ or TNFα (both 1:50) fluorochrome-conjugated monoclonal antibodies or with isotype-matched controls (Becton Dickinson, Wokingham, UK) for 45 min at RT. 5000 islet cells/pool or 100000 spleen cells/spleen were analysed on a BD LSRFortessa™ using BD FACSDiva™ software (BD Biosciences, Southampton, UK) and analysis was conducted with FlowJo (Tree Star). Gating strategies are shown in Supplemental Figure 3-9.

Preparation of reformed islets

2000-2500 islets isolated from BALB/c mice (Envigo, UK) were hand-picked from suspension cultures 24h after isolation and washed with PBS. Islets were then dissociated into a suspension of single cells through trypsin digestion. Trypsin digestion was stopped by adding neurobasal media consisting of MEM supplemented with 5% (v/v) FBS, 1x B-27, 1%(v/v) penicillin and streptomycin, HEPES 10 mM, Glutamax 1x, Na-pyruvate 1mM, and 11 mM glucose. Islet cells were seeded at a density of 35,000 cells/cm^2 on laminin-coated or collagenase-coated glass coverslips. Cells were then cultured for 3-4 days to allow adherence and spread on the glass surfaces, and for a further 10-14 days to form reformed islets (35).

Migration assays

Islets were isolated from BALB/c mice, and reformed islets were generated as described above. BALB/c mice express the MHC class H2Kd haplotype and are therefore matched to antigen-specific T cells. CD8+ cells were isolated from the spleens of 8-week-old diabetic female NY8.3 NOD mice (a kind gift from Dr James Pearson, Cardiff University). A single-cell suspension was prepared with MojoSort buffer at 1 × 10^8 cells/ml. 10 µl of biotinylated antibody containing antibodies against CD4, CD11b, CD11c, CD19, CD24, CD45R/B220, CD49b, CD105, I-A/I-E, TER-119/Erythroid, and TCRγδ were added. The mixture was then incubated for 15 min on ice, and 10

µL streptavidin nanobeads were added. The final volume of 120 µL of the cell and bead mixture was incubated on ice for an additional 15 min. Finally, 120 µL was diluted in 1x MojoSort buffer (2.5 mL) and placed in a MojoSort Magnet (Cat# 480019/480020, BioLegend) for 5 min for magnetic separation. The free cells in the solution were collected as enriched $CD8^+$ T cells.

The migration assay was conducted using an 8µm pore transwell plate (BioVision, Inc., USA) according to the manufacturer's protocol. BALB/c islets were incubated for 48h in 2% FBS RPMI complete medium in the lower chamber of a Transwell culture plate. Following this, $2X10^5$ $CD8^+$ T cells were seeded into the upper chamber and placed over coverslips with reformed islets treated with pro-inflammatory alone or in combination with FK866. After 18 h of incubation, the cells in the lower chamber were quantified by measuring the O.D values at Ex/Em = 540/590 nm using a PHERAstar Microplate Reader (35). Figure 6 shows a schematic representation of the experimental set-up.

Data analysis

Significance was tested using one- or two-way ANOVA with Tukey's hoc test, using GraphPad PRISM software (San Diego, CA, USA). Data are expressed as mean ± SEM. Experimenters were not blind to group assignment and outcome assessment.

Results

NAMPT inhibition protects mouse pancreatic islets from pro-inflammatory cytokine-induced dysfunction and human islets from cytokine-induced apoptosis

Beta-cell dysfunction and death in T1D is partly characterised by chronic exposure of beta-cells to pro-inflammatory cytokines. Cytokine-receptor ligation and subsequent signal transduction within beta cells results in their functional demise and/or reduced morphological mass. Given that NAMPT inhibition using FK866 or compound 17 decreases NMN and NAD+ levels in a cell-free environment, and in MIN6 cells and isolated mouse islets (Supplemental Fig. 1), we first investigated the impact of NAMPT inhibition on the deleterious effects of cytokine signalling in pancreatic mouse and human islets. Static glucose stimulated insulin secretion (GSIS) studies showed that both FK886 and compound 17 exerted significant protective effects against cytokine-mediated reductions in GSIS (both p=<0.0001 vs. Cytokines 1 ng/ml) (Fig. 1A and 1B). Neither FK866 (10 – 20 nM) nor compound 17 had any effects on static GSIS when added in the absence of cytokines (Supplemental Fig. 2). Co-incubation and pre-treatment with FK866 (Fig.

1C and Fig. 1D; p=<0.0001 vs. Cytokines 1 ng/ml) or compound 17 (Fig. 1E; P<0.001) also significantly protected against apoptosis (caspase 3/7 activity) in mouse islets. Finally, we observed that both FK866 and compound 17 also prevented cytokine-mediate apoptosis in human islets (Fig.1F).

FK866 protects pancreatic mouse islets from deleterious pro-inflammatory cytokine-mediated transcriptional changes

To understand how NAMPT activity impacts the deleterious effects of pro-inflammatory cytokines in greater detail, we conducted genome-wide transcriptome analysis on isolated mouse islets co-treated with cytokines and FK866 via bulk RNA sequencing (RNA-seq). Cytokine treatment led to the significant upregulation of 1873 genes and downregulation of 1718 genes (Fig. 2A). Gene set enrichment analysis (GSEA) revealed most elevated responses were downstream of cytokine activity (IFNγ signalling and TNF*α*+ signalling). Key beta cell functional and maturity genes were also downregulated (Fig. 2B and 2C). More in-depth analysis of the "Inflammatory response" gene sets illustrates many of the cytokine-induced significantly upregulated genes encode for proteins mediating or responding to inflammation and cellular stress. These include chemokines (*Ccl5*, *Cxcl10*, *Cxcl9*, *Ccl22*), cytokine receptor proteins (*Tnfsf10*, *Tnfrsf1b*, *Osmr*) and antigen processing and presenting proteins (*Tapbp, Cd40, Marco*) likely symbolising islet cells experiencing a pro-inflammatory response (Fig. 2D and 2E).

Compared to cytokine-treated islets, FK866 + cytokine treated islets had 43 and 287 upregulated and downregulated genes, respectively (Fig. 2F). Notably, the presence of FK866 in the treatment led islet cells to downregulate pathways related to leukocyte migration, as well as leukocyte and granulocyte chemotaxis. Interestingly, FK866 reversed cytokine-induced upregulation of the "Inflammatory response" gene set (Fig. 2G and 2H). Specifically, FK866 reversed the cytokine-induced expression of chemokines and chemokine receptors (Ccl20, Cxcl5, Cmklr1), cytokine receptor proteins (*Il10r*, *Il7r*, *Osmr*), and cytokines (*Il1b*, *Il6* and *Lif*), innate immune response genes (*Clec5a*, *Cybb*) (Fig. 2I). Leading edge analysis also exemplifies that FK866 supressed a pro-inflammatory response in islets (Fig. 2J).

NAMPT inhibition ameliorates hyperglycaemia and reductions in insulin content in MLDS-induced diabetic mice

Given that NAMPT activity played a role in cytokine-induced changes in beta-cell function and survival in vitro, and inhibiting NAMPT activity downregulated cytokine-induced upregulation of

genes associated with T1D autoimmune events (leukocyte migration and inflammatory response), we next sought to assess the effects of pharmacological NAMPT inhibition on the course of diabetes development *in vivo*. In vivo, effects on glycaemic control were observed in response to vehicle alone in C17 experiments (data not shown), hence these experiments were discontinued and only FK866 data is reported here. Diabetes was induced in mice by multiple-low dose streptozotocin (MLDS) administration (40 mg/kg bw; IP for 5 consecutive days). FK866 was administered to MLDS-induced diabetic mice, beginning at day 7 (two days after the end of STZ administration) as outlined in Fig. 3A. From day 11 until the end of the experiment (day 23), FK866 treatment significantly lowered (~25%) ambient blood glucose concentrations in $MLDS^{FK866}$ mice, compared to $MLDS^{Saline}$ and $MLDS^{Vehicle}$ treatment (Fig. 3B and 3C). FK866 administration also lowered fasting blood glucose levels in MLDS mice (Fig. 3D)

To determine whether improvements in glycaemic controls are related to improvements in beta-cell function, we assessed whether FK866 enhanced serum insulin and c-peptide response to glucose. $MLDS^{Saline}$ mice exhibited significantly lower plasma insulin ($p=0.05$) and C-peptide ($p=0.01$) compared to non-diabetic/CAB^{saline} animals. FK866 treatment slightly, but non-significantly, prevented MLDS-mediated reductions in insulin (Fig. 3E) and c-peptide secretion (3F, $p<0.08$). Beta cell health was examined in greater detail through assessment of insulin content per beta cell, using flow cytometry. MLDS induced a significant reduction in sub-population of granulated beta cells ($p=0.0001$) and a significant increase in sub-population of degranulated beta cells ($p=0.0001$). Consistent with a beta-cell protective effect, FK866 treatment led to a significant increase in proportion of granulated beta-cells ($p<0.05$) and a significant decrease in proportion of degranulated beta-cells ($p<0.05$) compared to the $MLDS^{Saline}$ (Fig. 3G). These findings suggest that pharmacological NAMPT inhibition with FK866 improves glycaemic control, in part through partial protection of beta-cell function and maintenance of beta-cell insulin content during MLDS-induced diabetes development.

NAMPT inhibition protects MLDS-induced diabetic mice from insulitis

We next sought to determine whether the effects of FK866 on glycaemic control early in the experimental period were linked to supressed insulitis. We initially examined this by histologically grading the severity of insulitis after 7 days FK866 administration (experimental day 14). Whilst all severities of insulitis were observed in $MLDS^{Saline}$ and $MLDS^{FK866}$ mice, $MLDS^{FK866}$ mice exhibited a greater proportion of islets that remained in the perivascular/periductal infiltration stage rather than progressing to the peri-insulitis/insulitis phase (Fig. 4A - C), indicating partial protection against insulitis by FK866.

To gain a deeper insight into these effects, the proportion of immune cell sub-types present within the islet was examined using flow cytometry. $MLDS^{Saline}$ mice displayed a significant ~2-fold increase of $CD4^+$ (p=0.05) and $CD8^+$T-cells (p<0.01), as well as $F4/80^+$macrophages (p<0.001), in the islet cell population compared to their non-diabetic counterparts, suggesting MLDS induces insulitis in these mice (Fig. 4D – F). Similar to the outcomes observed following H+E staining, FK866 administration led to a partial but non-significant decrease (~25%) in the proportion of $CD4^+$T-cells, $CD8^+$T-cells and $F4/80^+$macrophages in the islet population, compared to $MLDS^{Saline}$ mice (Fig. 4D - F). These results suggest that NAMPT may have an immunomodulatory role in impacting the intensity of insulitis during T1D development and that NAMPT inhibition partially reduced insulitis severity. A crucial factor in immune-mediated T1D pathophysiology is activation of immune cells leading to TNFα and IFNγ production which in turn mediate beta-cell destruction. To assess the effect of FK866 on immune cell activation, we began by measuring TNF*α* and IFNγ production within the intra-islet environment. $MLDS^{Saline}$ mice had significantly elevated proportions of $TNF\alpha^+$ cells in the total islet population compared to non-diabetic/CAB^{Saline} mice (p=0.05), and FK866 significantly blocked this effect (Fig. 4G; P<0.01). Assessment of immune sub-populations within all $TNF\alpha^+$ cells revealed $MLDS^{Saline}$ mice displayed significantly increased proportions of $TNF\alpha^+$CD4+ (P<0.05) and $TNF\alpha^+F4/80^+$ cells (P<0.001) compared to CAB^{Saline} mice, and these increases were blocked by FK866 (p=0.01 and p=0.001, respectively; Fig. 4H and 4I). When $IFN\gamma^+$ cells were measured, we $MLDS^{Saline}$ mice displayed significantly elevated proportions of $IFN\gamma^+$ cells in the total islet population (p<0.05; Supplemental Fig. 10A), and partial, but non-significant increases in $IFN\gamma^+$CD4+ and $IFN\gamma^+F4/80^+$ sub-populations (Supplemental Fig. 10A-D). FK866 administration led to small but non-significant reductions in these effects. Together this data demonstrates that NAMPT inhibition can prevent islet immune-cell activation, specifically by reducing TNFα production from $CD4^+$T-cells and $F4/80^+$macrophages. This provides a plausible mechanism through which FK866 prevents beta-cell destruction and improves glycaemic control in MLDS mice.

NAMPT inhibition reduces proliferation of splenic- and islet-derived immune cell proliferation in MLDS-induced diabetic mice

To further elucidate the immunomodulatory impact of NAMPT inhibition, we examined the effects of FK866 on proliferation of islet-derived $CD4^+$ and $CD8^+$ T-cells and $F4/80^+$ macrophages. $MLDS^{Saline}$ mice displayed significantly increased proportions of proliferating $CD4^+$, $CD8^+$ and $F4/80^+$ cells compared to non-diabetic mice (p=0.01, p=0.05 and p=0.05, respectively) (Fig. 5A-C). Consistent with an immunomodulatory beta-cell protective effect, FK866 prevented MLDS-induced increases in islet-derived $CD4^+$T-cells and $F4/80^+$ cells (Fig. 5A and 5B; p<0.05), but not

$CD8^+$T-cells (Fig. 5C). We also examined changes in splenocyte proliferation. $MLDS^{Saline}$ mice exhibited significantly elevated proportions of splenocyte proliferation compared to non-diabetic mice (p=0.05). The partial protective effects of FK866 are evident by the lack of significant increases in spontaneous splenocyte proliferation $MLDS^{FK866}$ mice when compared ND mice (Fig. 5D). Staining for immune cell sub-types within the splenocyte population revealed that FK866 also prevented MLDS-mediated increases in spontaneous proliferation of spleen-derived $CD4^+$ and $CD8^+$T-cells (P<0.05), (Fig. 5E-F). Together, these results demonstrate the clear anti-inflammatory, immunomodulatory effect of NAMPT inhibition on $CD4^+$ and $F4/80^+$ immune cells activation during T1D development.

NAMPT inhibition prevents cytotoxic $CD8^+$T-cell migration into pancreatic islets

To further examine the immunoregulatory effects of FK866, we utilised a transwell culture platform to assess the effect of FK866 on migration of CD8+T-cells obtained from NOD mice, into pancreatic islets (35). Exposure of islets to pro-inflammatory cytokines alone led to a 3-fold increase in CD8+T-cell migration compared to untreated islets (p<0.001). However, when islets were either pre-treated with FK866 prior to cytokine exposure, or co-incubated with FK866 and cytokines, these effects were completely blocked, with CD8+T-cell migration remaining at basal levels (p<0.001) (Fig.6).

Discussion

Here, we provide evidence that supports a role for NAMPT as an immunomodulatory enzyme which plays a key role in T1D pathogenesis. Of potential clinical importance, NAMPT inhibition leads to improved glycaemic control and beta-cell function during diabetes development in mice. These beneficial effects are driven in part by prevention of MLDS-induced insulitis and immune cell activation and by blocking the deleterious effects of pro-inflammatory cytokine signal transduction in islets.

Whilst FK866-mediated increases in insulin and c-peptide may appear modest, clinical studies have reported that type 1 diabetes patients with stimulated plasma C-peptide levels of as little as ≥ 0.02 pmol/mL (which is indicative of residual beta-cell function) exhibit improved metabolic control and lower insulin requirements, compared to T1D patients with C-peptide plasma levels below this threshold (36,37). This suggests that relatively small improvements in beta-cell function can lead to clinically relevant improvements in glycemic control in T1D. This strengthens the rationale that NAMPT inhibition may be an attractive therapeutic strategy to treat T1D.

NAMPT inhibition led to a reduction in insulitis, demonstrated by a marked reduction in MLDS-induced T-cell and macrophage islet infiltration. These effects are similar to those previously reported in studies of spinal cord injury, acute liver failure and myocardial infarction (38-40). Furthermore, FK866 treatment reportedly reduced colitis-induced chemokine and cell adhesion molecule expression in the DSS-induced colitis mouse model (24).

The GSEA performed in this study suggests that NAMPT activity is a positive regulator of cytokine-induced expression of genes that facilitate leukocyte migration and chemotaxis, which may explain the prohibitive effects on insulitis observed in response to pharmacological NAMPT inhibition *in vivo*. In addition to transcriptional changes, FK866 administration may also have an impact on the secretion of peptides that stimulate macrophage and leukocyte recruitment, and hence, insulitis (41). NAMPT exists in intra-cellular and extra-cellular forms, termed NAMPT and eNAMPT respectively. FK866 has been shown to block IFNγ- and TNFα-induced eNAMPT secretion from keratinocytes and fibroblasts. Moreover, eNAMPT sensitises TNFα-induced expression and secretion of CCL2, CXCL8, and IL6 which induce immune cell recruitment (42) and play a key role in insulitis (43-45). Conversely, eNAMPT secretion can be promoted by cytokines (46-48). We report that MLDS-induced diabetes development led to significantly increased IFNγ and TNFα islet levels. This suggests that MLDS-induced islet inflammation could mediate increased eNAMPT release within the local islet environment, which promotes insulitis via increased expression of CCL2, CXCL8, and/or IL6. Furthermore, FK866 treatment may block eNAMPT release and subsequent expression of immune cell recruitment molecules, which will reduce insulitis. However, further investigations into eNAMPT release from islet cells, and its role in the immunopathology of T1D are required investigate this potential mechanism.

In T1D, beta-cell mass is reduced by 70–80% at the time of diagnosis and the mode of destruction is attributed predominately to increased islet levels of IL1β, TNFα and IFNγ (49-51). NAMPT inhibition *in vivo* reduced MLDS-induced IFNγ and TNFα cytokine production in islet cells. This is in line with previous reports demonstrating that dysregulated NAD+ metabolism is essential for $CD4^{+}$T-cell IFNγ and TNFα secretion (52). Furthermore, we demonstrated that FK866 can prevent migration of NOD mouse derived $CD8^{+}$T-cells into pancreatic islets. Cytotoxic $CD8^{+}$T-cells are key drivers of T1D pathophysiology through mediation of beta-cell destruction and the ability of FK866 to block migration of these cells into islets suggests therapeutic utility of this compound. This effect of FK866 may have increased the survival and function of pancreatic beta cells, and hence, improved disease outcomes.

Elevated spontaneous proliferation of spleen-derived lymphocytes has been characterised as part of MLDS-induced diabetes pathophysiology (34). This effect, which was observed in our investigations, was blocked by pharmacological NAMPT inhibition. Moreover, islet infiltrating $CD4^+$T-cells and $F4/80^+$macrophages possessed increased proliferative capacity in MLDS-induced diabetic mice – effects which were also blocked by FK866. This is consistent with studies reporting FK866-mediated blocking of T-cell proliferation and survival *in vitro* (20). FK866 can also induce T-cell dysfunction by depleting intracellular ATP levels via impeding glycolysis, as less NAD+ can be fed into the cycle. Importantly, the T-cell receptor downstream signalling cascade is strongly dependent on ATP (53). These effects may be mediated through CD38 and CD157 mediated hydrolysis of NAD+ to create cADPR and NAADP. These metabolites can regulate cytoplasmic Ca^{2+} fluxes, leading to activation of signalling pathways critical for T-cell proliferation (54,55). Thus, FK866 may prevent increased $CD4^+$T-cell proliferation through indirectly reducing Ca^{2+} availability, and hence, the fuel required for proliferation.

Our data showed that FK866 led to protection against cytokine-induced reductions in GSIS in isolated mouse islets. It should be noted that a previous study conversely found that NMN administration, potentially via increased NAD synthesis, protected isolated mouse islets from cytokine-attenuated GSIS (56-59). However, this study, and others which have reported beneficial effects of NMN, have utilised pharmacological levels of NMN (~100 μM) several orders of magnitude greater than are observed physiologically. Therefore, it is difficult to compare the findings of these experiments with the current study, in which islet NMN levels were generally less than 10 μM across all treatment groups.

We report that NAMPT inhibition protects isolated mouse and human islets from cytokine-induced apoptosis. At first glance, these results are surprising as treating cancer cells with FK866 induces apoptosis following increased caspases-3/-7 activation (60). However, a recent study found that FK866 supressed caspase-3 activity in H_2O_2 stimulated-HeLa cells, but increased LDH release (a measure of necrosis) (61). The reasoning behind these findings is that as NAMPT activity regulates NAD+, and subsequently ATP levels; and because ATP fuels caspase-3 activation, NAMPT therefore plays a key role in determining whether cells undergo caspase-3-mediated apoptosis or caspase-3-independent necrosis. For pancreatic beta cells, changes within cytokine signalling, NAD+ salvage, and intracellular ATP levels could independently or concurrently factor into whether they survive or die. Thus, there may be an ideal, pharmacological level of NAMPT inhibition in pancreatic beta cells that prevents of extrinsic apoptosis pathway yet does not trigger necrosis. Further investigations are necessary to

elucidate the mechanisms linking intracellular NAD+ metabolism and beta cell survival. Moreover, whilst our data has focussed on the beta-cell protective role of FK866 in MLDS mice, non-pancreatic effects may also play a role. For example, gut inflammation and immune dysregulation are reported to play a role in diabetes onset and progression in MLDS mice, whilst FK866 has been shown to ameliorate gut inflammation in non-diabetic models (24). Further studies are required to elucidate potential non-pancreatic effects of FK866 in MLDS mice.

Conclusion

In summary, we characterise NAMPT as an immunoregulatory enzyme that plays a key role in autoimmune events observed in T1D development in mice. The data presented here acts as a clear proof-of-principle in identifying NAMPT inhibition as a novel intervention which can prevent autoimmune pathologies in T1D development.

References

(1) Bottini, N., Musumeci, L., Alonso, A., Rahmouni, S., Nika, K., Rostamkhani, M., MacMurray, J., Meloni, G.F., Lucarelli, P., Pellecchia, M., Eisenbarth, G.S., Comings, D., Mustelin, T., 2004. A functional variant of lymphoid tyrosine phosphatase is associated with type I diabetes. Nat. Genet. 36, 337–338. https://doi.org/10.1038/ng1323

(2) Chandra, R.K., 1997. Nutrition and the immune system: an introduction. Am. J. Clin. Nutr. 66, 460S-463S. https://doi.org/10.1093/ajcn/66.2.460S

(3) Erlich, H., Valdes, A.M., Noble, J., Carlson, J.A., Varney, M., Concannon, P., Mychaleckyj, J.C., Todd, J.A., Bonella, P., Fear, A.L., Lavant, E., Louey, A., Moonsamy, P., Type 1 Diabetes Genetics Consortium, 2008. HLA DR-DQ haplotypes and genotypes and type 1 diabetes risk: analysis of the type 1 diabetes genetics consortium families. Diabetes 57, 1084–1092. https://doi.org/10.2337/db07-1331

(4) Kaufman, F.R., 2000. Role of the Continuous Glucose Monitoring System in Pediatric Patients. Diabetes Technol. Ther. 2, 49–52. https://doi.org/10.1089/15209150050214122

(5) Nguyen, C., Varney, M.D., Harrison, L.C., Morahan, G., 2013. Definition of high-risk type 1 diabetes HLA-DR and HLA-DQ types using only three single nucleotide polymorphisms. Diabetes 62, 2135–2140. https://doi.org/10.2337/db12-1398

(6) Pugliese, A., 2016. Insulitis in the pathogenesis of type 1 diabetes. Pediatr. Diabetes 17, 31–36. https://doi.org/10.1111/pedi.12388

(7) Thomas, H.E., Irawaty, W., Darwiche, R., Brodnicki, T.C., Santamaria, P., Allison, J., Kay, T.W.H., 2004. IL-1 Receptor Deficiency Slows Progression to Diabetes in the NOD Mouse. Diabetes 53, 113–121. https://doi.org/10.2337/diabetes.53.1.113

(8) Wang, B., André, I., Gonzalez, A., Katz, J.D., Aguet, M., Benoist, C., Mathis, D., 1997. Interferon-gamma impacts at multiple points during the progression of autoimmune diabetes. Proc. Natl. Acad. Sci. U. S. A. 94, 13844–13849. https://doi.org/10.1073/pnas.94.25.13844

(9) Yoon, J.-W., Jun, H.-S., 2005. Autoimmune destruction of pancreatic beta cells. Am. J. Ther. 12, 580–591. https://doi.org/10.1097/01.mjt.0000178767.67857.63

(10) Cryer, P.E., Davis, S.N., Shamoon, H., 2003. Hypoglycemia in diabetes. Diabetes Care 26, 1902–1912. https://doi.org/10.2337/diacare.26.6.1902

(11) Jacobson, A.M., Braffett, B.H., Cleary, P.A., Gubitosi-Klug, R.A., Larkin, M.E., 2013. The Long-Term Effects of Type 1 Diabetes Treatment and Complications on Health-Related Quality of Life. Diabetes Care 36, 3131–3138. https://doi.org/10.2337/dc12-2109

(12) Shapiro, A.M.J., 2012. Islet Transplantation in Type 1 Diabetes: Ongoing Challenges, Refined Procedures, and Long-Term Outcome. Rev. Diabet. Stud. RDS 9, 385–406. https://doi.org/10.1900/RDS.2012.9.385

(13) Shapiro, A.M.J., Pokrywczynska, M., Ricordi, C., 2017. Clinical pancreatic islet transplantation. Nat. Rev. Endocrinol. 13, 268–277. https://doi.org/10.1038/nrendo.2016.178

(14) Garten, A., Schuster, S., Penke, M., Gorski, T., Giorgis, T. de, Kiess, W., 2015. Physiological and pathophysiological roles of NAMPT and NAD metabolism. Nat. Rev. Endocrinol. 11, 535–546. https://doi.org/10.1038/nrendo.2015.117

(15) Navas, L.E., Carnero, A., 2021. NAD+ metabolism, stemness, the immune response, and cancer. Signal Transduct. Target. Ther. 6, 1–20. https://doi.org/10.1038/s41392-020-00354-w

(16) Busso, N., Karababa, M., Nobile, M., Rolaz, A., Van Gool, F., Galli, M., Leo, O., So, A., De Smedt, T., 2008. Pharmacological Inhibition of Nicotinamide Phosphoribosyltransferase/Visfatin Enzymatic Activity Identifies a New Inflammatory Pathway Linked to NAD. PLoS ONE 3. https://doi.org/10.1371/journal.pone.0002267

(17) Ernst, I.M.A., Fliegert, R., Guse, A.H., 2013. Adenine Dinucleotide Second Messengers and T-lymphocyte Calcium Signaling. Front. Immunol. 4. https://doi.org/10.3389/fimmu.2013.00259

(18) Joseph, N., Reicher, B., Barda-Saad, M., 2014. The calcium feedback loop and T cell activation: How cytoskeleton networks control intracellular calcium flux. Biochim. Biophys. Acta BBA - Biomembr., Reciprocal influences between cell cytoskeleton and membrane channels, receptors and transporters 1838, 557–568. https://doi.org/10.1016/j.bbamem.2013.07.009

(19) Sandoval-Montes, C., Santos-Argumedo, L., 2005. CD38 is expressed selectively during the activation of a subset of mature T cells with reduced proliferation but improved potential to produce cytokines. J. Leukoc. Biol. 77, 513–521. https://doi.org/10.1189/jlb.0404262

(20) Bruzzone, S., Fruscione, F., Morando, S., Ferrando, T., Poggi, A., Garuti, A., D'Urso, A., Selmo, M., Benvenuto, F., Cea, M., Zoppoli, G., Moran, E., Soncini, D., Ballestrero, A., Sordat, B., Patrone, F., Mostoslavsky, R., Uccelli, A., Nencioni, A., 2009. Catastrophic NAD+ Depletion in Activated T Lymphocytes through Nampt Inhibition Reduces Demyelination and Disability in EAE. PLoS ONE 4. https://doi.org/10.1371/journal.pone.0007897

(21) Al-Shabany, A.J., Moody, A.J., Foey, A.D., Billington, R.A., 2016. Intracellular NAD+ levels are associated with LPS-induced TNF-α release in pro-inflammatory macrophages. Biosci. Rep. 36. https://doi.org/10.1042/BSR20150247

(22) Cameron, AM., Castoldi A., Sanin DE, Flachsmann LJ, Field CS, Puleston DJ, Kyle RL, Patterson AE, Hässler F, Buescher JM, Kelly B, Pearce EL, Pearce EJ, 2019. Inflammatory macrophage dependence on NAD+ salvage is a consequence of reactive oxygen species–mediated DNA damage Nature Immunology volume 20, pages420–432. DOI: 10.1038/s41590-019-0336-y

(23) Venter, G., Oerlemans, F.T.J.J., Willemse, M., Wijers, M., Fransen, J.A.M., Wieringa, B., 2014. NAMPT-mediated salvage synthesis of NAD+ controls morphofunctional changes of macrophages. PloS One 9, e97378. https://doi.org/10.1371/journal.pone.0097378

(24) Gerner, Romana R., Klepsch, V., Macheiner, S., Arnhard, K., Adolph, T.E., Grander, C., Wieser, V., Pfister, A., Moser, P., Hermann-Kleiter, N., Baier, G., Oberacher, H., Tilg, H., Moschen, A.R., 2018. NAD metabolism fuels human and mouse intestinal inflammation. Gut 67, 1813–1823. https://doi.org/10.1136/gutjnl-2017-314241

(25) Hasmann, M., Schemainda, I., 2003. FK866, a highly specific noncompetitive inhibitor of nicotinamide phosphoribosyltransferase, represents a novel mechanism for induction of tumor cell apoptosis. Cancer Res. 63, 7436–7442.

(26) Khan, J.A., Tao, X., Tong, L., 2006. Molecular basis for the inhibition of human NMPRTase, a novel target for anticancer agents. Nat. Struct. Mol. Biol. 13, 582–588.

(27) Gunzner-Toste et al, 2013; Discovery of potent and efficacious urea-containing nicotinamide phosphoribosyltransferase (NAMPT) inhibitors with reduced CYP2C9 inhibition properties. Bioorganic & Medicinal Chemistry Letters. Volume 23, Issue 12, 15 June 2013, Pages 3531-3538

(28) King, A.J., 2012. The use of animal models in diabetes research. Br. J. Pharmacol. 166, 877–894. https://doi.org/10.1111/j.1476-5381.2012.01911.x

(29) Formentini, L., Moroni, F., Chiarugi, A., 2009. Detection and pharmacological modulation of nicotinamide mononucleotide (NMN) in vitro and in vivo. Biochem. Pharmacol. 77, 1612–1620. https://doi.org/10.1016/j.bcp.2009.02.017

(30) Zhang, R.-Y., Qin, Y., Lv, X.-Q., Wang, P., Xu, T.-Y., Zhang, L., Miao, C.-Y., 2011. A fluorometric assay for high-throughput screening targeting nicotinamide phosphoribosyltransferase. Anal. Biochem. 412, 18–25. https://doi.org/10.1016/j.ab.2010.12.035

(31) Huang, G.C., Zhao, M., Jones, P., Persaud, S., Ramracheya, R., Löbner, K., Christie, M.R., Banga, J.P., Peakman, M., Sirinivsan, P., Rela, M., Heaton, N., Amiel, S., 2004a. The development of new density gradient media for purifying human islets and islet-quality assessments. Transplantation 77, 143–145. https://doi.org/10.1097/01.TP.0000100401.62912.B2

(32) Jones, P.M., Salmon, D.M., Howell, S.L., 1988. Protein phosphorylation in electrically permeabilized islets of Langerhans. Effects of Ca2+, cyclic AMP, a phorbol ester and noradrenaline. Biochem. J. 254, 397–403. https://doi.org/10.1042/bj2540397

(33) Pavlovic, S., Petrovic, I., Jovicic, N., Ljujic, B., Miletic Kovacevic, M., Arsenijevic, N., Lukic, M.L., 2018. IL-33 Prevents MLD-STZ Induction of Diabetes and Attenuate Insulitis in Prediabetic NOD Mice. Front. Immunol. 9. https://doi.org/10.3389/fimmu.2018.02646

(34) Luo, Z. *et al.* Kinetics of immune cell responses in the multiple low-dose streptozotocin mouse model of type 1 diabetes. *FASEB BioAdvances* **1**, 538–549 (2019).

(35) Haq N., Toczyska K.W., Wilson M.E, Jacobs M., Min Zhao, Lei Y., Shen Z, Pearson J., S.J. Persaud, Pullen T.J., Bewick G.A. Reformed islets: a long-term primary cell-based platform for exploring mouse and human islet biology. Cell Death Discov. 2024 Nov 23;10(1):480

(36) Lin, K., Yang, X., Wu, Y., Chen, S., Zeng, Q., 2021. Residual β-Cell Function in Type 1 Diabetes Followed for 2 Years after 3C Study. J. Diabetes Res. 2021, e9946874. https://doi.org/10.1155/2021/9946874

(37) Sørensen, J.S., Johannesen, J., Pociot, F., Kristensen, K., Thomsen, J., Hertel, N.T., Kjaersgaard, P., Brorsson, C., Birkebaek, N.H., the Danish Society for Diabetes in Childhood and Adolescence, 2013. Residual β-Cell Function 3–6 Years After Onset of Type 1 Diabetes Reduces Risk of Severe Hypoglycemia in Children and Adolescents. Diabetes Care 36, 3454–3459. https://doi.org/10.2337/dc13-0418

(38) Guo, E., Li, R., Yang, J., Zhang, J., Li, A., Yang, Y., Liu, S., Liu, A., Jiang, X., 2017. FK866 attenuates acute hepatic failure through c-jun-N-terminal kinase (JNK)-dependent autophagy. Sci. Rep. 7, 2206. https://doi.org/10.1038/s41598-017-02318-7

(39) Esposito, E., Impellizzeri, D., Mazzon, E., Fakhfouri, G., Rahimian, R., Travelli, C., Tron, G.C., Genazzani, A.A., Cuzzocrea, S., 2012. The NAMPT inhibitor FK866 reverts the damage in spinal cord injury. J. Neuroinflammation 9, 66. https://doi.org/10.1186/1742-2094-9-66

(40) Montecucco, F., Bauer, I., Braunersreuther, V., Bruzzone, S., Akhmedov, A., Lüscher, T.F., Speer, T., Poggi, A., Mannino, E., Pelli, G., Galan, K., Bertolotto, M., Lenglet, S., Garuti, A., Montessuit, C., Lerch, R., Pellieux, C., Vuilleumier, N., Dallegri, F., Mage, J., Sebastian, C., Mostoslavsky, R., Gayet-Ageron, A., Patrone, F., Mach, F., Nencioni, A., 2013. Inhibition of Nicotinamide Phosphoribosyltransferase Reduces Neutrophil-Mediated Injury in Myocardial Infarction. Antioxid. Redox Signal. 18, 630–641. https://doi.org/10.1089/ars.2011.4487

(41) Roep, B.O., Peakman, M., 2011. Diabetogenic T lymphocytes in human Type 1 diabetes. Curr. Opin. Immunol. 23, 746–753. https://doi.org/10.1016/j.coi.2011.10.001

(42) Mercurio, L., Morelli, M., Scarponi, C., Scaglione, G.L., Pallotta, S., Avitabile, D., Albanesi, C., Madonna, S., 2021. Enhanced NAMPT-Mediated NAD Salvage Pathway Contributes to Psoriasis Pathogenesis by Amplifying Epithelial Auto-Inflammatory Circuits. Int. J. Mol. Sci. 22, 6860. https://doi.org/10.3390/ijms22136860

(43) DiCosmo, B.F., Picarella, D., Flavell, R.A., 1994. Local production of human IL-6 promotes insulitis but retards the onset of insulin-dependent diabetes mellitus in non-obese diabetic mice. Int. Immunol. 6, 1829–1837. https://doi.org/10.1093/intimm/6.12.1829

(44) Matos, M., Park, R., Mathis, D., Benoist, C., 2004. Progression to islet destruction in a cyclophosphamide-induced transgenic model: a microarray overview. Diabetes 53, 2310–2321. https://doi.org/10.2337/diabetes.53.9.2310

(45) Pan, X., Kaminga, A.C., Kinra, S., Wen, S.W., Liu, H., Tan, X., Liu, A., 2022. Chemokines in Type 1 Diabetes Mellitus. Front. Immunol. 12, 690082. https://doi.org/10.3389/fimmu.2021.690082

(46) Kieswich, J., Sayers, S.R., Silvestre, M.F., Harwood, S.M., Yaqoob, M.M., Caton, P.W., 2016. Monomeric eNAMPT in the development of experimental diabetes in mice: a potential target for type 2 diabetes treatment. Diabetologia 59, 2477–2486. https://doi.org/10.1007/s00125-016-4076-3

(47) Moschen, A.R., Kaser, A., Enrich, B., Mosheimer, B., Theurl, M., Niederegger, H., Tilg, H., 2007. Visfatin, an Adipocytokine with Proinflammatory and Immunomodulating Properties. J. Immunol. 178, 1748–1758. https://doi.org/10.4049/jimmunol.178.3.1748

(48) Sayers S.R., Beavil R.L., Fine N.H.F., Huang G.C., Choudhary P., Pacholarz K.J. Structure-functional changes in eNAMPT at high concentrations mediate mouse and human beta cell dysfunction in type 2 diabetes. Diabetologia. 2020 Feb;63(2):313–323.

(49) Cnop, M., Welsh, N., Jonas, J.-C., Jörns, A., Lenzen, S., Eizirik, D.L., 2005. Mechanisms of Pancreatic β-Cell Death in Type 1 and Type 2 Diabetes: Many Differences, Few Similarities. Diabetes 54, S97–S107. https://doi.org/10.2337/diabetes.54.suppl_2.S97

(50) Mathis, D., Vence, L., Benoist, C., 2001. β-Cell death during progression to diabetes. Nature 414, 792–798. https://doi.org/10.1038/414792a

(51) Padgett, L.E., Broniowska, K.A., Hansen, P.A., Corbett, J.A., Tse, H.M., 2013. The role of reactive oxygen species and proinflammatory cytokines in type 1 diabetes pathogenesis. Ann. N. Y. Acad. Sci. 1281, 16–35. https://doi.org/10.1111/j.1749-6632.2012.06826.x

(52) Tullius, S.G., Biefer, H.R.C., Li, S., Trachtenberg, A.J., Edtinger, K., Quante, M., Krenzien, F., Uehara, H., Yang, X., Kissick, H.T., Kuo, W.P., Ghiran, I., de la Fuente, M.A., Arredouani, M.S., Camacho, V., Tigges, J.C., Toxavidis, V., El Fatimy, R., Smith, B.D., Vasudevan, A., ElKhal, A., 2014. NAD+ protects against EAE by regulating CD4+ T-cell differentiation. Nat. Commun. 5. https://doi.org/10.1038/ncomms6101

(53) Wang, Y., Wang, F., Wang, L., Qiu, S., Yao, Y., Yan, C., Xiong, X., Chen, X., Ji, Q., Cao, J., Gao, G., Li, D., Zhang, L., Guo, Z., Wang, R., Wang, H., Fan, G., 2021. NAD+ supplement potentiates tumor-killing function by rescuing defective TUB-mediated NAMPT transcription in tumor-infiltrated T cells. Cell Rep. 36, 109516. https://doi.org/10.1016/j.celrep.2021.109516

(54) Guse, A.H., da Silva, C.P., Berg, I., Skapenko, A.L., Weber, K., Heyer, P., Hohenegger, M., Ashamu, G.A., Schulze-Koops, H., Potter, B.V., Mayr, G.W., 1999. Regulation of calcium signalling in T lymphocytes by the second messenger cyclic ADP-ribose. Nature 398, 70–73. https://doi.org/10.1038/18024

(55) Morra, M., Zubiaur, M., Terhorst, C., Sancho, J., Malavasi, F., 1998. CD38 is functionally dependent on the TCR/CD3 complex in human T cells. FASEB J. Off. Publ. Fed. Am. Soc. Exp. Biol. 12, 581–592. https://doi.org/10.1096/fasebj.12.7.581

(56) Caton, P.W., Kieswich, J., Yaqoob, M.M., Holness, M.J., Sugden, M.C., 2011. Nicotinamide mononucleotide protects against pro-inflammatory cytokine-mediated impairment of mouse islet function. Diabetologia 54, 3083–3092. https://doi.org/10.1007/s00125-011-2288-0

(57) Ramsey, K.M., Mills, K.F., Satoh, A., Imai, S., 2008. Age-associated loss of Sirt1-mediated enhancement of glucose-stimulated insulin secretion in beta cell-specific Sirt1-overexpressing (BESTO) mice. Aging Cell 7, 78–88. https://doi.org/10.1111/j.1474-9726.2007.00355.x

(58) Revollo, J.R., Körner, A., Mills, K.F., Satoh, A., Wang, T., Garten, A., Dasgupta, B., Sasaki, Y., Wolberger, C., Townsend, R.R., Milbrandt, J., Kiess, W., Imai, S., 2007. Nampt/PBEF/visfatin regulates insulin secretion in β cells as a systemic NAD biosynthetic enzyme. Cell Metab. 6, 363–375. https://doi.org/10.1016/j.cmet.2007.09.003

(59) Yoshino, J., Mills, K.F., Yoon, M.J., Imai, S., 2011. Nicotinamide mononucleotide, a key NAD(+) intermediate, treats the pathophysiology of diet- and age-induced diabetes in mice. Cell Metab. 14, 528–536. https://doi.org/10.1016/j.cmet.2011.08.014

(60) Gehrke, I., Bouchard, E.D.J., Beiggi, S., Poeppl, A.G., Johnston, J.B., Gibson, S.B., Banerji, V., 2014. On-Target Effect of FK866, a Nicotinamide Phosphoribosyl Transferase Inhibitor, by Apoptosis-Mediated Death in Chronic Lymphocytic Leukemia Cells. Clin. Cancer Res. 20, 4861–4872. https://doi.org/10.1158/1078-0432.CCR-14-0624

(61) Nishida, T., Naguro, I., Ichijo, H., 2022. NAMPT-dependent NAD+ salvage is crucial for the decision between apoptotic and necrotic cell death under oxidative stress. Cell Death Discov. 8, 1–11. https://doi.org/10.1038/s41420-022-01007-3

Acknowledgements

We thank J. I. Miyazaki (Osaka University, Osaka, Japan) for provision and consent to use MIN6 cells. Flow cytometric analysis was conducted in the Biomedical Research Centre Advanced Flow Cytometry Platform at King's College London (London, UK). Library generated for RNA sequencing was conducted by the Genomics Centre at King's College London. Human islets were provided through the King's College London Human Islet Research Tissue Bank (KCL HI-RTB; 20/SW/0074). We thank the families of the pancreas donors and the Cell Therapy Unit in the NIHR/Wellcome King's Clinical Research Facility at that houses the clinical islet isolation laboratory for making islets available for this research. D.E. was recipient of a King's Medical Research Trust PhD studentship. This work was also supported by an EFSD/Lilly European Diabetes Research Programme grant and Diabetes UK project grants (18/0005865; 20/0006297). The study funders were not involved in the design of the study; the collection, analysis, and interpretation of data; writing the report; or the decision to submit the report for publication.

Author contributions

DE, SRS, NH, JJV, SB, VKL, ELH, LS, HG, JK, TJP, KJP, DH, MZ, SB, JG, JP, GB, SJP and PWC designed and conducted research, analysed data, and reviewed and approved the final manuscript. DE and PWC wrote the paper. PWC is the guarantor of this work.

Conflict of Interest

None declared.

Figures and Legends

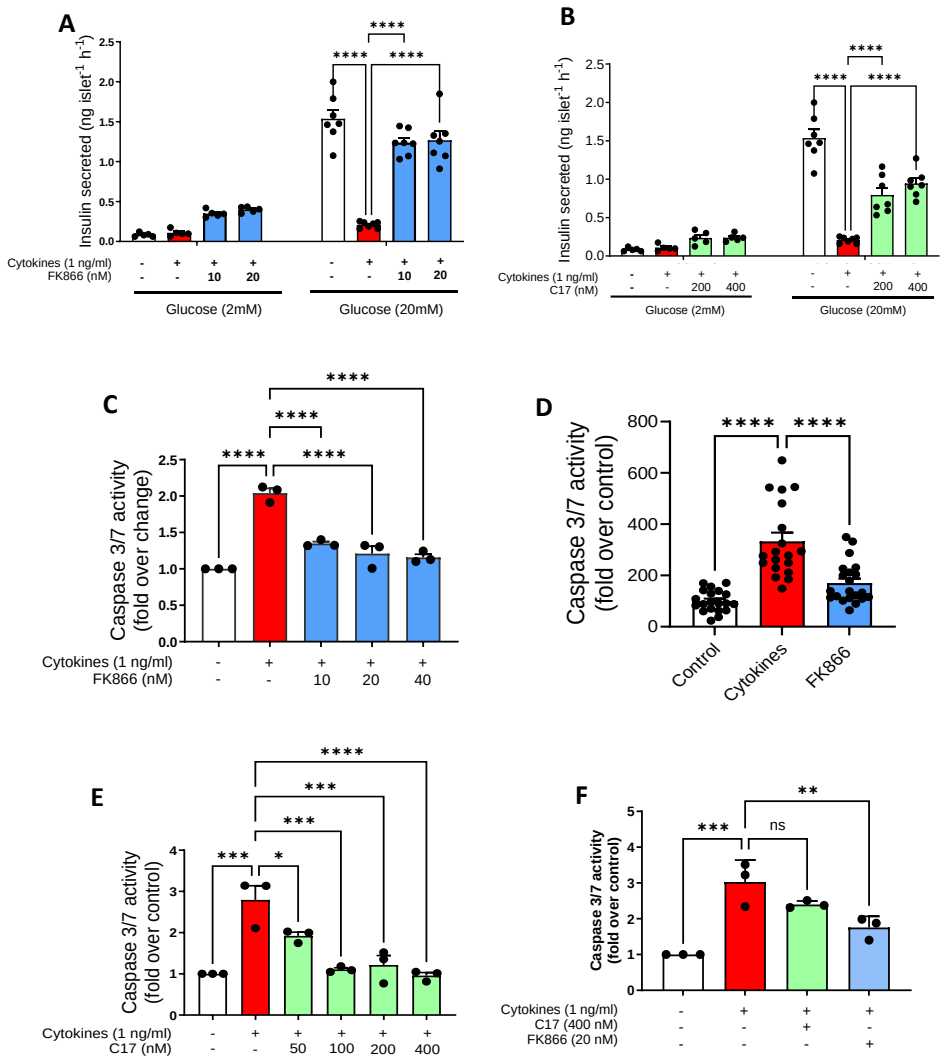

Fig. 1. NAMPT inhibition exerts protective effects against pro-inflammatory cytokine-induced beta-cell dysfunction and apoptosis in isolated pancreatic islets. (A-B) Static insulin secretion in response to basal (2mM) or 20mM glucose was assessed in isolated mouse islets incubated with cytokines (CK; IL-1β, TNFα and IFNγ; 1 ng/ml), with or without either **(A)** FK866 (10 – 20 nM) or **(B)** compound 17 (200 – 400 nM) for 24 h. N = 5 – 7 replicates from 6 mice and representative of three independent experiments. **(C-D)** Apoptosis (caspase 3/7 activity) was measured in isolated mouse islets treated with **(C)** CK cocktail with or without FK866 (10 – 40 nM) for 24 h, or **(D)** in mouse islet treated with FK866 (10 nM) for 2 h followed by CK treatment (without FK866) for 22 h. **(E)** Apoptosis (caspase 3/7 activity) measured in isolated mouse islets treated with CK cocktail with or without compound 17 (50 – 400 nM) for 24 h. For C-E, n = 3 where an n of 1 is equal one experiment with 10 wells, each with five size-matched islets. **(F)** Apoptosis (caspase 3/7 activity) measured in isolated human islets treated with a CK cocktail with or without either FK866 (20 nM) or compound 17 (400 nM) for 24 h. n = 3 where an n of 1 is equal one experiment with 10 wells, each with five size-matched islets. Values in all graphs are represented as means ± SEM. Statistical significance between groups is depicted by *p < 0.05, **p<0.01; **p<0.001 ****p < 0.0001.

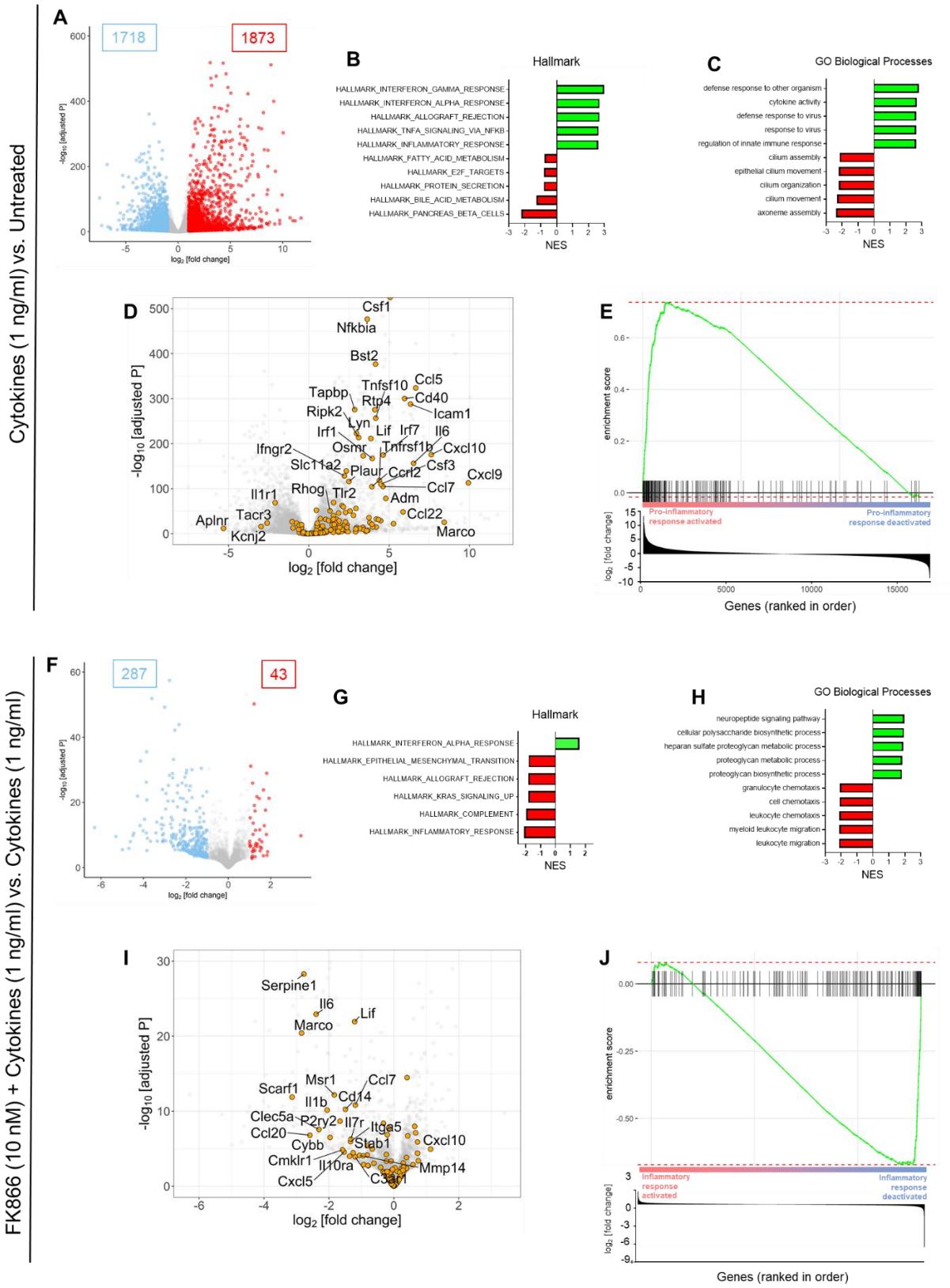
Cytokines (1 ng/ml) vs. Untreated
A
1718
1873
-log10 [adjusted P]
log2 [fold change]
B
Hallmark
HALLMARK_INTERFERON_GAMMA_RESPONSE
HALLMARK_INTERFERON_ALPHA_RESPONSE
HALLMARK_ALLOGRAFT_REJECTION
HALLMARK_TNFA_SIGNALING_VIA_NFKB
HALLMARK_INFLAMMATORY_RESPONSE
HALLMARK_FATTY_ACID_METABOLISM
HALLMARK_E2F_TARGETS
HALLMARK_PROTEIN_SECRETION
HALLMARK_BILE_ACID_METABOLISM
HALLMARK_PANCREAS_BETA_CELLS
NES
C
GO Biological Processes
defense response to other organism
cytokine activity
defense response to virus
response to virus
regulation of innate immune response
cilium assembly
epithelial cilium movement
cilium organization
cilium movement
axoneme assembly
NES
D
Csf1
Nfkbia
Bst2
Tnfsf10
Ccl5
Tapbp
Rtp4
Cd40
Ripk2
Icam1
Lyn
Irf1
Lif
Irf7
Il6
Ifngr2
Osmr
Tnfrsf1b
Cxcl10
Slc11a2
Plaur
Ccrl2
Csf3
Cxcl9
Rhog
Tlr2
Ccl7
Il1r1
Adm
Aplnr
Tacr3
Ccl22
Kcnj2
Marco
-log10 [adjusted P]
log2 [fold change]
E
enrichment score
Pro-inflammatory response activated
Pro-inflammatory response deactivated
log2 [fold change]
Genes (ranked in order)
FK866 (10 nM) + Cytokines (1 ng/ml) vs. Cytokines (1 ng/ml)
F
287
43
-log10 [adjusted P]
log2 [fold change]
G
Hallmark
HALLMARK_INTERFERON_ALPHA_RESPONSE
HALLMARK_EPITHELIAL_MESENCHYMAL_TRANSITION
HALLMARK_ALLOGRAFT_REJECTION
HALLMARK_KRAS_SIGNALING_UP
HALLMARK_COMPLEMENT
HALLMARK_INFLAMMATORY_RESPONSE
NES
H
GO Biological Processes
neuropeptide signaling pathway
cellular polysaccharide biosynthetic process
heparan sulfate proteoglycan metabolic process
proteoglycan metabolic process
proteoglycan biosynthetic process
granulocyte chemotaxis
cell chemotaxis
leukocyte chemotaxis
myeloid leukocyte migration
leukocyte migration
NES
I
Serpine1
Il6
Lif
Marco
Msr1
Ccl7
Scarf1
Cd14
Il1b
Clec5a
P2ry2
Il7r
Itga5
Ccl20
Cxcl10
Cybb
Stab1
Cmklr1
Il10ra
Mmp14
Cxcl5
C3ar1
-log10 [adjusted P]
log2 [fold change]
J
enrichment score
Inflammatory response activated
Inflammatory response deactivated
log2 [fold change]
Genes (ranked in order)

Fig. 2. FK866 suppresses cytokine-induced inflammatory transcriptional pathway enrichment in isolated pancreatic mouse islets. (A and F) Volcano plot depicting log2 fold changes of differentially expressed (DE) annotated genes from RNA-seq performed on isolated mouse islets treated for 24 h with (A) a cytokine cocktail (IL-1β, TNFα and IFNγ; 1 ng/ml) versus untreated, or **(B)** FK866 (10 nM) and a cytokine cocktail versus a cytokine cocktail. Each dot represents a gene. DE genes with a log2 fold change of >1, all adjusted $P < 0.05$ are highlighted in red (indicating upregulation) or blue (indicating downregulation). Numbers denote total number of upregulated and downregulated genes between treatment groups. **(C,B,G,H)** Five most and least enriched pathways as revealed by gene set enrichment analysis (GSEA) in isolated mouse islets treated for 24 h with (C and B) a CK cocktail versus untreated, or **(G and H)** FK866 (10 nM) and a cytokine cocktail versus a cytokine cocktail. GSEA performed with **(C,G)** 'Hallmark' and **(B,H)** 'Gene Ontology (GO) biological processes' gene sets from the Molecular Signatures Database (MSigDB). Only gene sets with significant ($p < 0.05$) normalised enrichment scores shown. **(D and I)** Volcano plot depicting log2 fold changes of DE genes within the 'HALLMARK_INFLAMMATORY_RESPONSE' gene set. The annotated genes are from RNA-seq performed on isolated mouse islets treated for 24 h with **(D)** a CK cocktail versus untreated, or (I) FK866 (10 nM) and a cytokine cocktail versus a cytokine cocktail. Each dot represents a gene. Gene names are displayed for top differentially expressed genes (log2 fold change >1, adjusted $P < 0.05$). **(E and J)** Enrichment plots derived from the GSEA performed on the transcripts within the 'HALLMARK_INFLAMMATORY_RESPONSE' gene set in isolated mouse islets treated for 24 h with **(E)** a CK cocktail versus untreated, or **(J)** FK866 (10 nM) and a cytokine cocktail versus a cytokine cocktail. Green line denotes running statistic and black lines represent a single gene in the gene set. Bottom left figures are bar plots showing all DE genes log2 fold changes ranked in order. n=3 independent biological sample replicates (each replicate consisted of 150 islets).

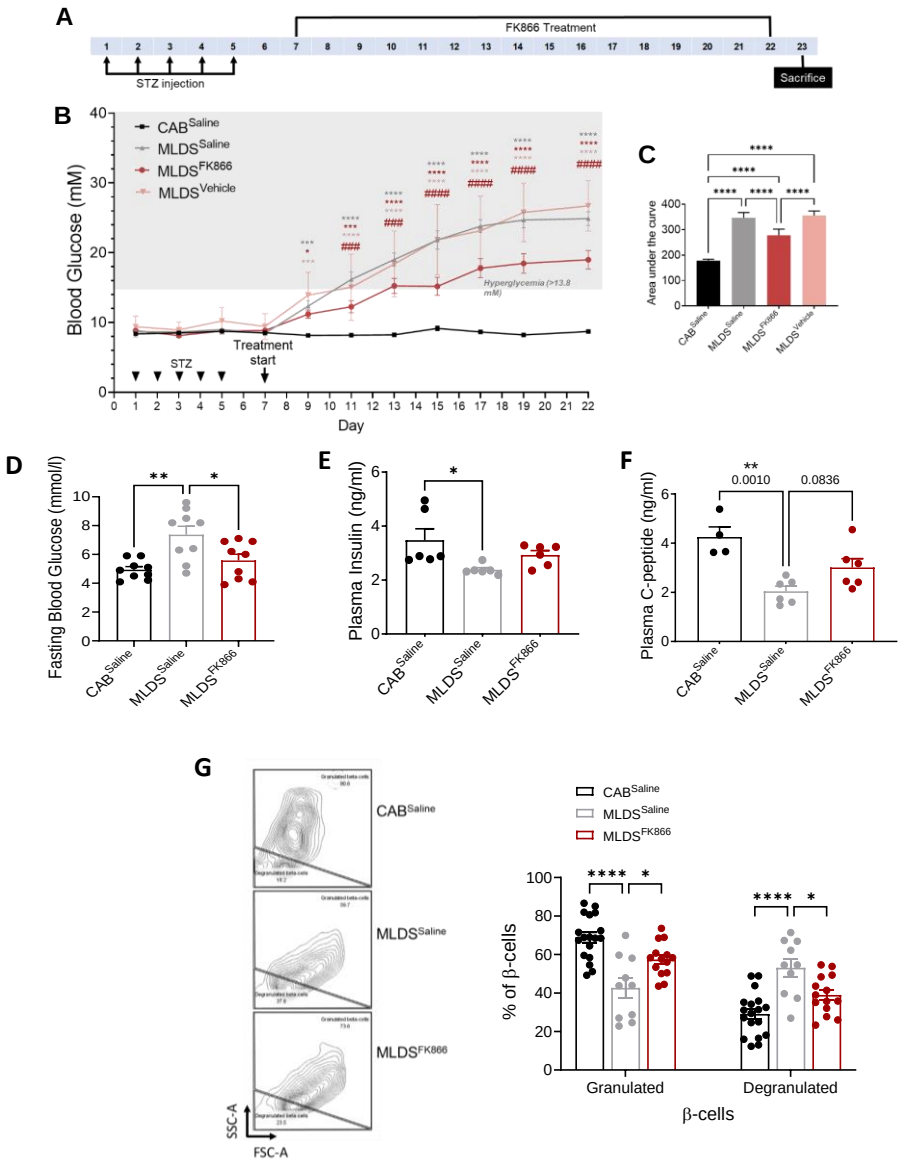

Fig. 3. FK866 ameliorates MLDS-induced hyperglycaemia and reduced beta-cell functionality. (A) Schematic diagram of the experimental protocol: mice were administered citric acid buffer (CAB) or multiple low dose streptozotocin (MLDS) regimen, then after 48 hours, were administered saline, FK866 or vehicle (IP) for 17 days. **(B and C)** Ambient blood glucose measured every 2-3 days and the corresponding comparison of areas under the curves. In left panel, black arrows and annotations denote streptozotocin (STZ) exposure and FK866 treatment (n = 12-29). **(D)** Fasting blood glucose (day 23); **(E and F)** Plasma levels of insulin and C-peptide measured though ELISA using terminal blood samples taken on the day of sacrifice (day 23) following 24 h fast and then injection of 2 g/kg 30% glucose solution (n = 6). **(G)** Representative image of data showing SSC/FCS of granulated and degranulated β cells on the day of sacrifice (day 23). Also shown are corresponding percentages of the optical properties of insulin-positive islet cells following isolation, dispersion and immunofluorescence staining of insulin. n = 14-18 pools of islet cells of which a maximum of 5000 cells were analysed. Values in all graphs are represented as means ± SEM. Statistical significance vs CABSaline is depicted by *p < 0.05, **p < 0.01, ***p < 0.001, ****p < 0.0001. Statistical significance vs MLDSSaline is depicted by #p < 0.05, ##p < 0.01, ###p < 0.001, ####p < 0.0001.

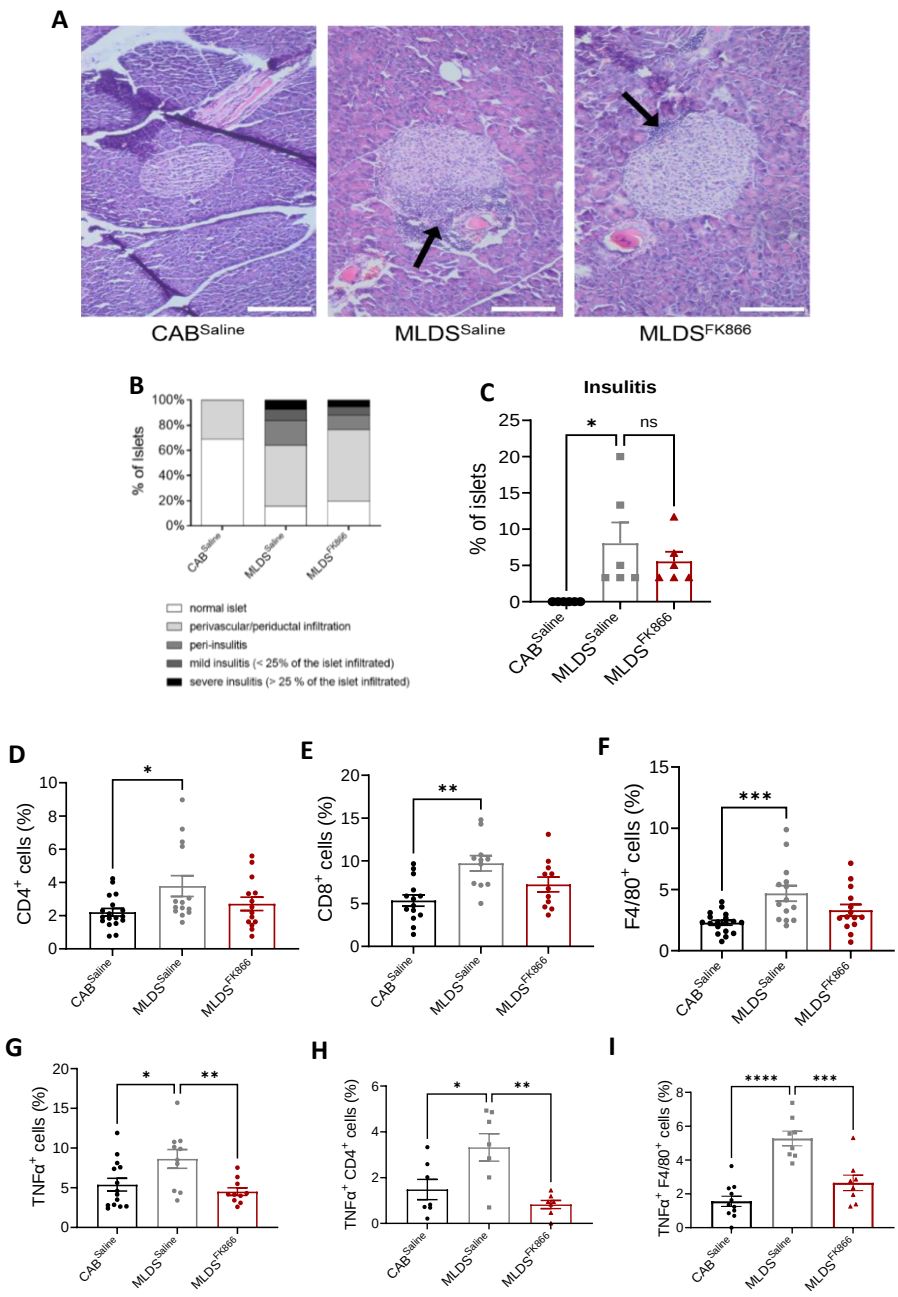

Fig. 4. FK866 partially protects MLDS-induced diabetic mice from insulitis.

(A) Representative images of mouse pancreas from CAB^{Saline}, MLDS^{Saline} and MLDS^{FK866} mice stained with hematoxylin and eosin and evaluated for severity of infiltrating immune cells using light microscopy. Black arrows indicate immune cell infiltration. Imaged at 20× (Scale bars, 50 μM). **(B)** Corresponding percentages of islets graded for all stages of insulitis. **(C)** Percentages of islets showing mild and severe insulitis only. Data generated from 60 islets per mouse pancreas (three mice per group). **(D-F)** Percentage of **(D)** CD4$^+$, **(E)** CD8$^+$ and **(F)** F4/80$^+$ cells within the islet cell population of CAB^{Saline}, MLDS^{Saline} and MLDS^{FK866} mice following sacrifice. n = 14-18 pools of islets of which a maximum of 5000 cells were analysed. **(G-I)** Percentages of **(G)** TNFα+, **(H)** TNFα+CD4+, **(I)** TNFα+F4/80+, within the islet cell of CAB^{Saline}, MLDS^{Saline} and MLDS^{FK866} mice. n = 7-14 pools of islets of which a maximum of 5000 cells were analysed. Values in all graphs are represented as means ± SEM. Statistical significance is depicted by *p < 0.05, **p < 0.01, ***p < 0.001, ****p<0.0001.

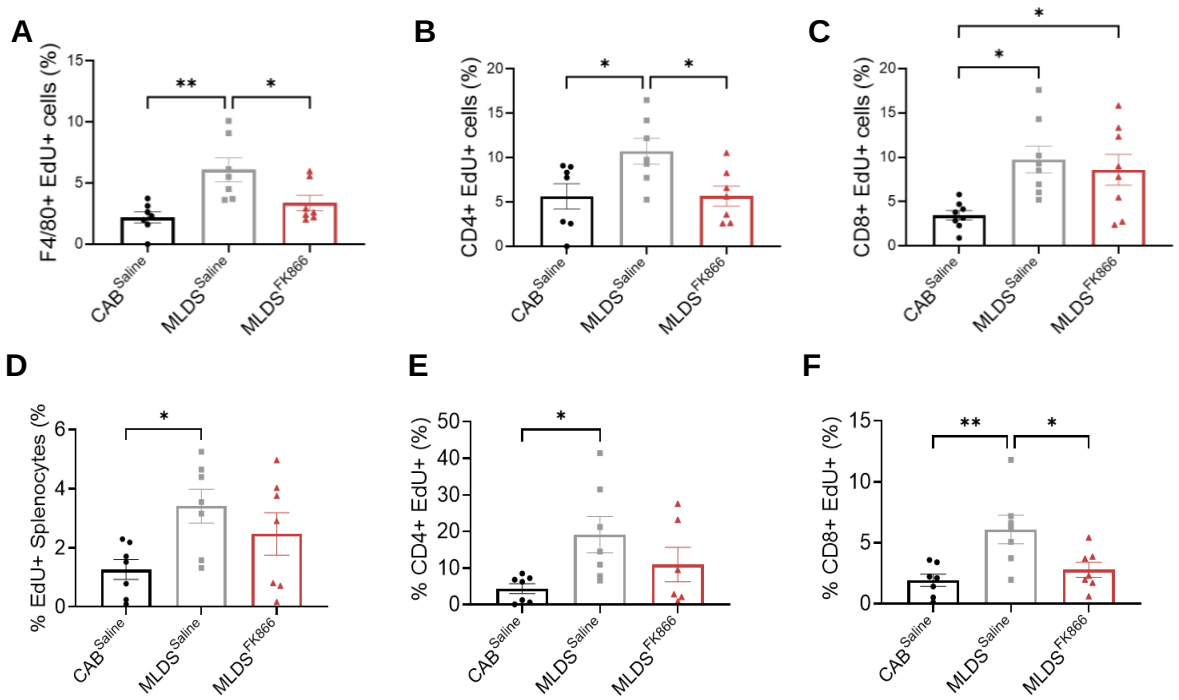

Fig. 5. FK866 blocks MLDS-mediated increased proliferation of islet- and spleen derived immune cells. (A-C) Percentages of **(A)** $CD4^{+}EdU^{+}$, **(B)** $CD8^{+}EdU^{+}$, **(C)** $F4/80^{+}EdU^{+}$ cells within the islet cell population of CAB^{Saline}, $MLDS^{Saline}$ and $MLDS^{FK866}$ mice following sacrifice, pancreatic islet isolation, dispersion, EdU-supplemented culture (72 h) staining and flow cytometric analysis. **(D-F)** Percentages of **(D)** EdU^{+} splenocytes, **(E)** $CD4^{+}EdU^{+}$, **(F)** $CD8^{+}EdU^{+}$ cells within the splenocyte population of CAB^{Saline}, $MLDS^{Saline}$ and $MLDS^{FK866}$ mice following sacrifice, spleen removal, dispersion, culture with EdU (24 h), staining and flow cytometric analysis. n = 7-8 pools of islet or spleen cells of which a maximum of 5000 cells were analysed. Values in all graphs are represented as means ± SEM. Statistical significance is depicted by *$p < 0.05$, **$p < 0.01$.

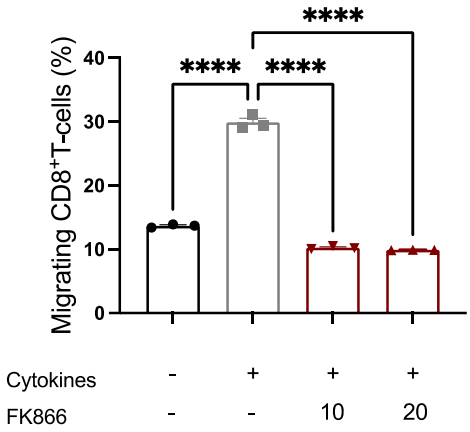

Fig. 6. FK866 prevents migration of cytotoxic CD8⁺T-cells into pancreatic islets. (A) Schematic diagram of the experimental protocol. Islets were isolated from BALB/c mice and dispersed and reaggregated into reformed islets. CD8+T-cells were isolated from splenocytes derived from NY8.3 NOD mice. **(B)** Islets were exposed to pro-inflammatory cytokines (IL-1β, TNFα and IFNγ; 1 ng/ml), with or without FK866 (10 – 20 nM) for 18 h. Migration of CD8+ cells into islets was assessed using a transwell culture platform. Values in all graphs are represented as means ± SEM. Statistical significance is depicted by ****$p < 0.0001$.